

## 2.5. ELECTRON DIFFRACTION AND ELECTRON MICROSCOPY IN STRUCTURE DETERMINATION

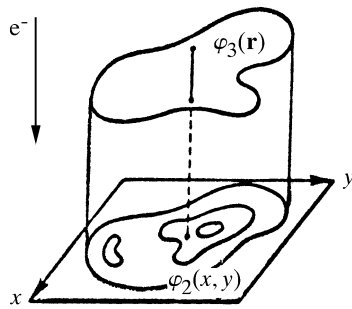


Fig. 2.5.6.1. A three-dimensional object  $\varphi_3$  and its two-dimensional projection  $\varphi_2$ . The electron beam penetrates the specimen in the direction of the  $z$  axis.

The projection direction is defined by a unit vector  $\boldsymbol{\tau}(\theta, \psi)$  and it is formed on the plane  $\mathbf{x}$  perpendicular to  $\boldsymbol{\tau}$ . The set of various projections  $\varphi_2(\mathbf{x}_\tau) = \varphi_2(\mathbf{x}_i)$  may be assigned by a discrete or continuous set of points on a unit sphere  $|\boldsymbol{\tau}| = 1$  (Fig. 2.5.6.2).

In Fourier space, the relation between an object and its projection is referred to as the central section theorem: the Fourier transformation of projection  $\varphi_2$  of a 3D object  $\varphi_3$  is the central (*i.e.*, passing through the origin of reciprocal space) 2D plane cross section of a 3D transform perpendicular to the projection vector (Bracewell, 1956; DeRosier & Klug, 1968; Crowther, Amos *et al.*, 1970). In Cartesian coordinates, a 3D Fourier transform is

$$\begin{aligned} \mathcal{F}[\varphi_3(\mathbf{r})] &= \Phi_3(u, v, w) \\ &= \iiint \varphi_3(x, y, z) \exp\{2\pi i(ux + vy + wz)\} dx dy dz. \end{aligned} \quad (2.5.6.6)$$

The transform of projection  $\varphi_2(x, y)$  along  $z$  is

$$\begin{aligned} \mathcal{F}[\varphi_2(x, y)] &= \Phi_3(u, v, 0) \\ &= \iiint \varphi_3(x, y, z) \exp\{2\pi i(ux + vy + 0z)\} dx dy dz \\ &= \iint \varphi_3(x, y, z) dz \exp\{2\pi i(ux + vy)\} dx dy \\ &= \iint \varphi_2(x, y) \exp\{2\pi i(ux + vy)\} dx dy \\ &= \Phi_2(u, v). \end{aligned} \quad (2.5.6.7)$$

In the general case of projecting along the vector  $\boldsymbol{\tau}$ , the central section theorem is

$$\mathcal{F}[\varphi_2(\mathbf{x}_\tau)] = \Phi_3(\mathbf{u}_\tau), \quad \mathbf{u}_\tau \perp \boldsymbol{\tau}. \quad (2.5.6.8)$$

From this theorem it follows that the inversion of the 3D ray transform is possible if there is a continuous set of projections  $\varphi_\tau$  corresponding to the motion of the vector  $\boldsymbol{\tau}(\theta, \psi)$  over any continuous line connecting the opposite points on the unit sphere (Fig. 2.5.6.2) (Orlov's condition: Orlov, 1976). This result is evidenced by the fact that in this case the cross sections  $\mathcal{F}[\varphi_2(\mathbf{x}_\tau)]$  that are perpendicular to  $\boldsymbol{\tau}$  in Fourier space continuously cover the whole Fourier space, *i.e.*, they yield  $\mathcal{F}[\varphi_3(\mathbf{r})]$  and thereby determine  $\varphi_3(\mathbf{r}) = \mathcal{F}^{-1}[\Phi_3(\mathbf{u})]$ .

In single-particle reconstruction, imaged objects are randomly and nonuniformly oriented on the substrate at different angles (Frank, 2006) and the distribution of their orientations is beyond our control; therefore, the practical impact of Orlov's condition is limited. In fact, it is more useful to determine *a posteriori*, *i.e.*, after the 3D reconstruction of the macromolecule is computed, how well the Fourier space was covered. This can be done by calculating the distribution of the 3D spectral signal-to-noise ratio (Penczek, 2002).

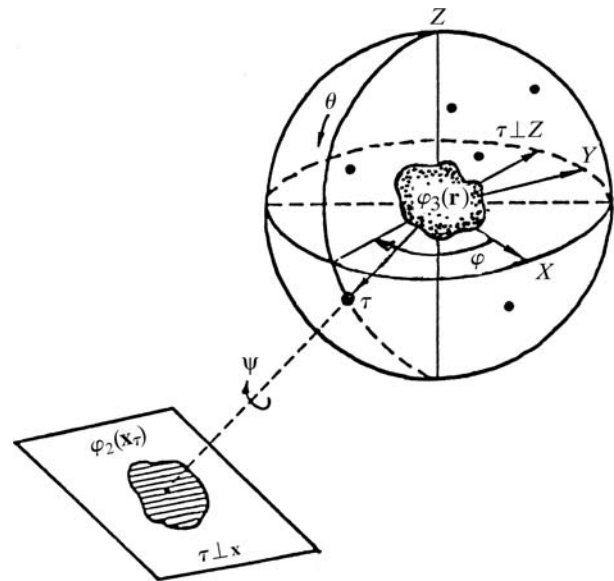


Fig. 2.5.6.2. The projection sphere and projection  $\varphi_2(\mathbf{x}_\tau)$  of  $\varphi_3(\mathbf{r})$  along  $\boldsymbol{\tau}$  onto the plane  $\boldsymbol{\tau} \perp \mathbf{x}$ . The case  $\boldsymbol{\tau} \perp Z$  represents orthoaxial projection. Points indicate an arbitrary distribution of projection directions  $\boldsymbol{\tau}$ .

## 2.5.6.2. 3D reconstruction in the general case

In the general case of the 3D reconstruction of  $\varphi_3(\mathbf{r})$  from projections  $\varphi_2(\mathbf{x}_\tau)$ , the projection vector  $\boldsymbol{\tau}$  occupies arbitrary positions on the projection sphere (Fig. 2.5.6.2). First, let us consider the case of a 2D function  $\rho_2(\mathbf{x})$  and its ray transform  $\varphi_1(x, \psi)$ . We introduce an operation of backprojection  $b$ , which is stretching along  $\boldsymbol{\tau}_\psi$  each 1D projection  $\varphi_1(x_\psi)$  (Fig. 2.5.6.3). When the result is integrated over the full angular range of projections  $\varphi_1(x, \psi)$ , we obtain the projection synthesis defined as

$$b(x, y) = \int_0^\pi \varphi_1(x \cos \psi + y \sin \psi, \psi) d\psi. \quad (2.5.6.9)$$

However, the backprojection operator is not the inverse of a 2D ray transform, as the resulting image  $b$  is blurred by the point-spread function  $(x^2 + y^2)^{-1/2}$  (Vainshtein, 1971):

$$b(x, y) = \rho(x, y) * (x^2 + y^2)^{-1/2}. \quad (2.5.6.10)$$

By noting that the Fourier transform of  $(x^2 + y^2)^{-1/2}$  is  $(u^2 + v^2)^{-1/2}$  and by using the convolution theorem  $\mathcal{F}[f * g] = \mathcal{F}[f]\mathcal{F}[g]$ , we obtain the 'backprojection-filtering' inversion formula:

$$\begin{aligned} \rho(x, y) &= b(x, y) * (x^2 + y^2)^{1/2} = \mathcal{F}^{-1}[\mathbf{u}|\mathcal{F}[b]] \\ &= \text{Filtration}_{|\mathbf{u}|}[\text{Backprojection}(\varphi_1)]. \end{aligned} \quad (2.5.6.11)$$

The more commonly used 'filtered-backprojection' inversion is based on the 2D version of the central section theorem (2.5.6.8):

$$\mathcal{F}[\varphi_1(x_\psi)] = \Upsilon_2(\mathbf{u}_\psi) = \Upsilon_2(R, \Psi), \quad (2.5.6.12)$$

where  $\mathcal{F}[\rho_2] = \Upsilon_2$ . With this in mind,  $\rho_2(\mathbf{x})$  can be related to its ray transform by evaluating the Fourier transform of  $\rho_2$  in polar coordinates: